

The Positive Capacity Region of Two-Dimensional Run-Length-Constrained Channels

Keren Censor and Tuvi Etzion, *Fellow, IEEE*

Abstract—A binary sequence satisfies a one-dimensional (d, k) constraint if every run of zeros (with possible exception of the first and the last runs) has length at least d and at most k . A binary two-dimensional array satisfies a (d, k) constraint if each row and each column satisfies the one-dimensional (d, k) constraint. Few models have been proposed in the literature to handle two-dimensional data: the diamond model, the square model, the hexagonal model, and the triangular model. The constraints in the different directions might be asymmetric and hence many kind of constraints are defined depending on the number of directions in the model. For example, a two-dimensional array in the diamond model satisfies a (d_1, k_1, d_2, k_2) constraint if it satisfies the one-dimensional (d_1, k_1) constraint horizontally and the one-dimensional (d_2, k_2) constraint vertically. In this correspondence, the region in which the capacity is zero or positive, in the various models, is examined. Asymmetric constraints in the diamond model and symmetric constraints in the other models are considered. In particular, an almost complete solution for asymmetric constraints in the diamond model is provided.

Index Terms—Asymmetric constraints, capacity, constrained codes, diamond model, hexagonal model, permutation arrays, square model, tiling, triangular model, two-dimensional coding.

I. INTRODUCTION

Runlength constraint coding is widely used in digital storage applications, particularly magnetic and optical storage devices [8], [9]. Recent developments in optical storage—especially in the area of holographic memory—increase recording density by exploiting the fact that the recording device is a surface. In this new model, the recorded data is regarded as two-dimensional, as opposed to the track-oriented one-dimensional recording paradigm. This new approach, however, necessitates the introduction of new types of constraints which are two-dimensional rather than one-dimensional. While the one-dimensional case has been widely explored, results in the two-dimensional case have been slower to arrive. This is mainly due to the fact that imposing constraints in a few directions makes the coding problem much more difficult. Nevertheless, in the last decade there has been a considerable progress in the study of two-dimensional constraints.

A one-dimensional binary sequence is said to satisfy a (d, k) constraint if there are at least d zeros and at most k zeros between any pair of consecutive ones. Before the first one and after the last one, there are at most k zeros. A two-dimensional surface is said to satisfy a (d, k) constraint if each direction defined by its connectivity model satisfies a one-dimensional (d, k) constraint. The capacity of a two-dimensional constraint Θ is defined by

$$C(\Theta) = \lim_{n, m \rightarrow \infty} \frac{\log_2 N(n, m | \Theta)}{rnm}$$

where $N(n, m | \Theta)$ is the number of $n \times m$ arrays satisfying the constraint Θ . The number of points in an $n \times m$ array for the given

Manuscript received January 10, 2006; revised February 7, 2006. The material in this correspondence was presented in part in the 2006 IEEE International Symposium on Information Theory, Seattle, WA, July 2006.

The authors are with the Department of Computer Science, Technion-Israel Institute of Technology, Technion City, Haifa 32000, Israel (e-mail: ckeren@cs.technion.ac.il; etzion@cs.technion.ac.il).

Communicated by M. Sudan, Associate Editor for Coding Theory.

Digital Object Identifier 10.1109/TIT.2006.883544

connectivity model is rnm . An array which satisfies the constraint Θ is called Θ constrained or a Θ array.

Data should be organized on a two-dimensional surface in some order. This order will be defined by the way in which the data is read. For this purpose, four connectivity models are defined. The diamond model, the square model, and the hexagonal model are frequently considered in the literature, e.g., for constrained codes they were considered first by Weeks and Blahut [18]. The triangular model was considered by [14] for constrained codes and for other applications in [5]. Some other papers which consider capacities of constraints in such models are [1], [6], [10], [11], [15], [16].

The first connectivity model is the *diamond* model. In this model, a point $(i, j) \in \mathbb{Z}^2$ has the following four neighbors:

$$\{(i+1, j), (i-1, j), (i, j+1), (i, j-1)\}.$$

When (i, j) is a boundary point, the neighbor set is reduced to points within the array. In this model, the data is organized in the two-dimensional rectangular grid and it is read horizontally and vertically.

The second model is called the *square* model, in which each point $(i, j) \in \mathbb{Z}^2$ has eight neighbors

$$\{(i+1, j), (i-1, j), (i, j+1), (i, j-1), \\ (i+1, j+1), (i-1, j+1), (i+1, j-1), (i-1, j-1)\}.$$

In this model, the data is organized in the two-dimensional rectangular grid and it is read horizontally, vertically, and in the two diagonal directions.

The third model is called the *hexagonal* model. Instead of the rectangular grid we have used up to now, we define the following graph. We start by tiling the plane \mathbb{R}^2 with regular hexagons. The vertices of the graph are the center points of the hexagons. These points define the hexagonal lattice [4]. We connect two vertices if and only if their respective hexagons are adjacent. In this way, each vertex has exactly six neighboring vertices.

We will use an isomorphic representation of the model. This representation includes \mathbb{Z}^2 as the set of vertices. Each point $(i, j) \in \mathbb{Z}^2$ has the following neighboring vertices:

$$\{(i+1, j), (i-1, j), (i, j+1), \\ (i, j-1), (i-1, j-1), (i+1, j+1)\}.$$

It may be shown that the two models are isomorphic [17]. From now on, by abuse of notation, we will also call the last model—the hexagonal model. In this isomorphic model, the data is organized in the two-dimensional rectangular grid and it is read horizontally, vertically, and in the direction of one of the diagonals called *right diagonal*.

All the neighbor sets of the three different models are summarized in Fig. 1. A square with a dot is the point (i, j) . In all models, rows and columns of the arrays will be indexed in ascending order, bottom to top and left to right.

The fourth model is called the *triangular* model. Again, we start by tiling the plane \mathbb{R}^2 with regular hexagons. The vertices of the graph are the vertices of the hexagons. The edges between the vertices are the sides of the hexagons. Hence, each vertex has exactly three neighboring vertices. If we connect the centers of the hexagons with lines we will obtain a tiling of the \mathbb{R}^2 with equilateral triangles. The vertices of the graph are the center points of the equilateral triangles. The set of vertices is also a union of two translates of the hexagonal lattice. Clearly, a point in this model can be represented by a triple $(i, j, s) \in \mathbb{Z}^2 \times \{0, 1\}$. Each point $(i, j, 0) \in \mathbb{Z}^2 \times \{0\}$ has the following neighboring vertices:

$$\{(i, j, 1), (i-1, j, 1), (i, j-1, 1)\}.$$

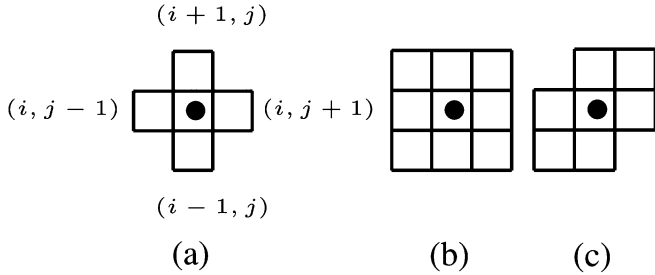


Fig. 1. Neighbors of position (i, j) in the (a) diamond model, (b) square model, (c) hexagonal model.

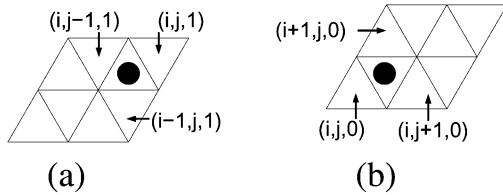


Fig. 2. Neighbors in the triangular model of positions $(i, j, 0)$ and $(i, j, 1)$.

Each point $(i, j, 1) \in \mathbb{Z}^2 \times \{1\}$ has the following neighboring vertices:

$$\{(i, j, 0), (i + 1, j, 0), (i, j + 1, 0)\}.$$

The neighbor sets in this model are illustrated in Fig. 2.

As the vertices are two translates of the hexagonal lattice, one can consider the model as having six directions. We will consider it slightly different. Instead of data stored in the centers of the triangles, the data will occupy the whole area of the triangle. Therefore, in this interpretation there are three directions in this model. Finally, we note that in the triangular model an $n \times m$ array has $2nm$ points.

Let $C_{\diamond}(d, k)$ denote the capacity of the (d, k) two-dimensional constraint in the diamond model. Kato and Zeger [10] proved that $C_{\diamond}(d, k) > 0$ if and only if $k > d + 1$. $C_{\diamond}(d_1, k_1, d_2, k_2)$ denotes the capacity of the asymmetric (d_1, k_1, d_2, k_2) constraint in the diamond model, i.e., horizontally the constraint is (d_1, k_1) and vertically the constraint is (d_2, k_2) . These constraints were handled in [11]. $C_{\square}(d, k)$, $C_{\square}(d, k)$, $C_{\triangle}(d, k)$, denote the capacity of the (d, k) constraint in the square model, hexagonal model, and triangular model, respectively.

The rest of this correspondence is organized as follows. In Section II, we present the known basic techniques to prove zero or positive capacity. We generalize these techniques, so that they could be applied to more complicated cases which we will have in succeeding sections. In Section III, we examine asymmetric constraints in the diamond model and provide an almost complete solution for the zero/positive capacity region problem. In Sections IV–VI, we examine capacities of constraints in the square model, hexagonal model, and triangular model, respectively. Discussion and open problems are in Section VII.

II. BASIC TECHNIQUES

In this section, we will survey the known techniques, except for *ad hoc* methods, used to prove zero capacity and those used to prove positive capacity. We will generalize these techniques in a way that will enable them to handle more complicated scenarios. The first lemma which appeared in [11] is an immediate consequence of the definition of the (d, k) constraint.

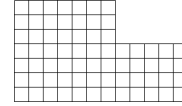


Fig. 3. A $[7 \times 12, 3 \times 5]$ skeleton tile.

Lemma 1: Let Θ be a constraint with minimum run-length d and maximum run-length k in direction Δ . Let $\tilde{\Theta}$ be a constraint with minimum run-length $\tilde{d} \leq d$ and maximum run-length $\tilde{k} \geq k$ in direction Δ and the same constraints, as in Θ , in the other directions. Then $C(\Theta) \leq C(\tilde{\Theta})$.

A. Positive Capacity

An $[n \times m, k \times \ell]$ skeleton tile is a tile which consists of an $n \times m$ array from which a $k \times \ell$ array was removed from the upper right corner. If $\ell = 1$ we simply have an $[n \times m, k]$ skeleton tile. An example of a $[7 \times 12, 3 \times 5]$ skeleton tile is given in Fig. 3.

For two points $z_1 = (x_1, y_1)$ and $z_2 = (x_2, y_2)$, $z_1, z_2 \in \mathbb{Z}^2$ let

$$\mathcal{L}(z_1, z_2) = \{(ix_1 + jx_2, iy_1 + jy_2) : i, j \in \mathbb{Z}\}$$

be the set of points spanned by z_1, z_2 . This is the lattice defined by z_1 and z_2 (see [4], [7]). Note, that by abuse of notation the first coordinate is for the row index and the second is for the column index. The following lemma can be easily verified.

Lemma 2: Let \mathcal{A} be an $[n \times m, k \times \ell]$ skeleton tile. If we place the bottom leftmost point of \mathcal{A} on the points of $\mathcal{L}((n-k, m-\ell), (n, -\ell))$ then a tiling of \mathbb{Z}^2 with copies of \mathcal{A} is obtained.

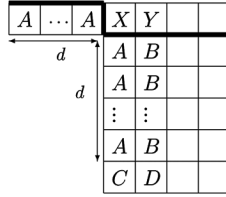
The tiling obtained by Lemma 2 will be called the *standard tiling*. If \mathcal{A} is an $n \times m$ array (a *skeleton array*), then the standard tiling is obtained by substituting $k = 0$ and $\ell = 0$ in the skeleton tile of Lemma 2. Clearly, we can also use a parallelogram instead of a rectangle. A standard tiling can use a few tiles with the same shape and different labels. In this case, each one of the tiles can have any one of the labels. The next lemma is a straightforward generalization of similar lemmas for skeleton arrays, given in [6], [11].

Lemma 3: Let \mathcal{A} and \mathcal{B} be two identical tiles with different labels, and Θ a two-dimensional constraint. If the standard tiling with \mathcal{A} and \mathcal{B} yields a two-dimensional array which is Θ constrained then $C(\Theta) > 0$. Moreover, if we can use t identical tiles with different labels $\mathcal{A}_1, \dots, \mathcal{A}_t$ and the number of points in \mathcal{A}_i is N then $C(\Theta) \geq \frac{1}{N} \log_2 t$.

B. Zero Capacity

The most effective method to prove zero capacity was given by Blackburn [2] for specific constraints. However, the method can be formulated to handle general two-dimensional constraints.

Assume we want to show that the capacity of a two-dimensional constraint Θ is zero. We consider an $(n + r_1 + r_2) \times (m + t_1 + t_2)$ array \mathcal{A} which is Θ constrained, where t_1, t_2, r_1 , and r_2 are constants which might depend on the run-length constraints, but do not depend on n and m . Assume further that the labels at positions of the first r_1 rows, the last r_2 rows, the first t_1 columns, and the last t_2 columns, are known. We now scan the other positions of \mathcal{A} . We scan the other n rows from bottom to top, and the m positions in a row are scanned from left to right. We assume that all positions in the array are scanned, i.e., we omit labels which lead to positions which cannot be labeled. If each position is determined by the known labels and the positions which are already scanned then the capacity of the constraint Θ is *zero*. We will not give a proof to the claim since we will prove a much stronger result.

Fig. 4. Scanning of a $(d, d + 1)$ array.

This technique will be called *scanning*. The strength of scanning is demonstrated by providing a very short proof to the following theorem by Kato and Zeger [10].

Theorem 1: $C_{\diamond}(d, d + 1) = 0$.

Proof: Consider an $n \times m$ array \mathcal{A} which is $(d, d + 1)$ constrained. We will show that the labels of \mathcal{A} are determined by the labels at positions (i, j) , where $0 \leq i \leq d$ or $0 \leq j \leq d - 1$ or $j = m - 1$.

We will show that for every $d + 1 \leq i, d \leq j \leq m - 2$, the label of the position marked by X (see Fig. 4) is determined by the labels to the left of it and the labels below it. Assume to the contrary that X can be a zero and can be a one. It implies that all the positions marked by A are zeros and either X or Y is a one. Since Y can be a one, it follows that all positions marked by B are zeros. Since X can be a zero it follows by the vertical constraint that C is a one. Similarly, since Y can be a zero, it follows that D is a one, a contradiction to the horizontal constraint. Hence, $C_{\diamond}(d, d + 1) = 0$. \square

The scanning technique can be applied on all the connectivity models. It is strengthened, to all connectivity models, as follows.

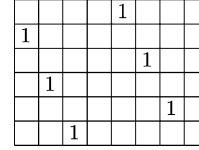
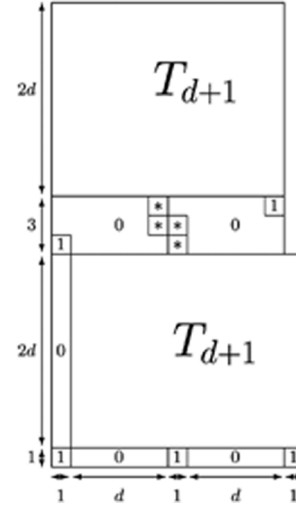
Theorem 2: Assume the scanning method is applied to a two-dimensional constraint Θ . If for the label in each position (i, j) scanned, one of the following three states holds:

- (s1) the label in position (i, j) is completely determined;
- (s2) the label can be either zero or one, but with one of these labels the suffix of the row is completely determined;
- (s3) the label can be either zero or one, but the prefix of the row before position (i, j) is a given sequence $\mathcal{P}(i, j)$; then $C(\Theta) = 0$.

Proof: Assume ρ positions, numbered by $0, 1, \dots, \rho - 1$, are scanned in a row. Let \mathcal{T} be a directed tree with $\rho + 1$ levels defined as follows. The root of \mathcal{T} (level 0) represents position 0. The vertices in level ℓ , $\ell < \rho$, represent position ℓ . The vertices in level ρ represent all the valid labels of all the ρ positions in the row. A vertex v which is not a leaf has out-degree one or two depending whether the label of the corresponding position is completely determined or not, respectively. The edge which connects a vertex v in level ℓ to vertex u in level $\ell + 1$ is labeled with one of the possible labels of the position represented by v . If the out-degree of v is two, then one edge is labeled by a zero and one edge is labeled by a one. Each vertex v is labeled with the ordered labels of the path from the root to v .

First, we note that the label on a vertex v , which represents position (i, j) , represents the labels of the positions before position (i, j) . If state (s3) holds in position (i, j) represented by v then the label on v must be $\mathcal{P}(i, j)$. Therefore, in each level there is at most one vertex which represents a position in which state (s3) holds. The number of leaves of a subtree whose root is in level ℓ and does not have vertices which represent positions in state (s3) is at most $\rho - \ell + 1$.

Now, we construct a tree \mathcal{T}' from \mathcal{T} by swapping subtrees of \mathcal{T} , with roots on the same level. Clearly, the number of leaves in \mathcal{T}' is equal the number of leaves in \mathcal{T} . \mathcal{T}' will be constructed in a way that

Fig. 5. The array T_4 .Fig. 6. The skeleton tile for the $(d, 2d + 1, 2d, 2d + 1)$ constraint.

all vertices which correspond to positions in which state (s3) holds, are on the same path. The total number of leaves of \mathcal{T}' , which are not on this path, is at most $\sum_{\ell=1}^{\rho} (\rho - \ell + 1) = \frac{(\rho+1)\rho}{2}$.

The number of leaves in \mathcal{T} is equal to the number of different labels for a row in the $(n + r_1 + r_2) \times (m + t_1 + t_2)$ array which is Θ constrained. It is now a simple exercise to compute the capacity and obtain $C(\Theta) = 0$. \square

III. ASYMMETRIC RUN-LENGTH-CONSTRAINED CHANNELS

Kato and Zeger [11] have considered the zero/positive region of $C_{\diamond}(d_1, k_1, d_2, k_2)$. They have summarized their results in which seven cases remained unsolved:

- (u1) $d_1 = 1, k_1 = 3, d_2 = 2, k_2 = 3$;
- (u2) $2 \leq d_1, k_1 = d_1 + 1, d_2 = d_1, k_2 \leq 2d_2$;
- (u3) $2 \leq d_1, d_1 + 2 \leq k_1 \leq 2d_1, d_2 = d_1, k_2 = d_2 + 1$;
- (u4) $2 \leq d_1, d_1 + 2 \leq k_1 \leq 2d_1, d_1 < d_2 < k_1 - 1, k_2 = d_2 + 1$;
- (u5) $2 \leq d_1, d_1 + 2 \leq k_1 \leq 2d_1, d_2 = k_1 - 1, k_2 \leq 2d_2$;
- (u6) $2 \leq d_1, 2d_1 < k_1, d_1 < d_2 < k_1 - 1, k_2 = d_2 + 1$;
- (u7) $2 \leq d_1, 2d_1 < k_1, d_2 = k_1 - 1, k_2 \leq 2d_2$.

In this section we will solve most of these cases.

Lemma 4: $C_{\diamond}(d, 2d + 1, 2d, 2d + 1) > 0$ for every $d \geq 1$.

Proof: Let T_n be a $(2n - 2) \times (2n)$ array defined as follows. $T_n(1, 2n - 2) = 1$ and $T_n(0, n - 2) = 1$; if $T_n(i, j) = 1$ then $T_n(i + 2, j - 1) = 1$ provided that $i + 2 \leq 2n - 3$. In all other positions T_n has zeros. T_4 is illustrated in Fig. 5.

Consider the $[(4d + 4) \times (2d + 3), 2d + 3]$ skeleton tile shown in Fig. 6. Let \mathcal{A} and \mathcal{B} be the two $[(4d + 4) \times (2d + 3), 2d + 3]$ tiles obtained from this skeleton tile by substituting the two skew tetriminoes shown in Fig. 7 instead of the four asterisks. We claim that any standard tiling with the arrays \mathcal{A} and \mathcal{B} yields a $(d, 2d + 1, 2d, 2d + 1)$ constrained array.

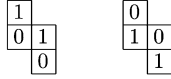


Fig. 7. Two skew tetrominoes for substitution in the skeleton tile.

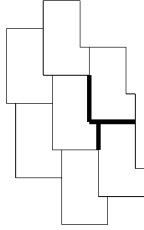
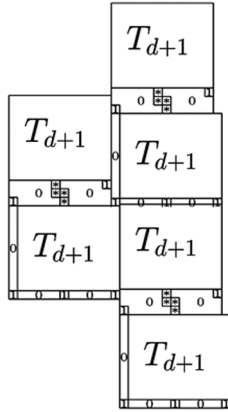


Fig. 8. Tiling the plane with skeleton tiles.


 Fig. 9. Areas crossing two tiles for the $(d, 2d+1, 2d, 2d+1)$ constraint.

One can easily verify that it is sufficient to prove that the $[(4d+4) \times (2d+3), 2d+3]$ skeleton tile is a $(d, 2d+1, 2d, 2d+1)$ tile and that the constraint is not violated on rows and columns crossing two different skeleton tiles on the positions marked in bold in Fig. 8.

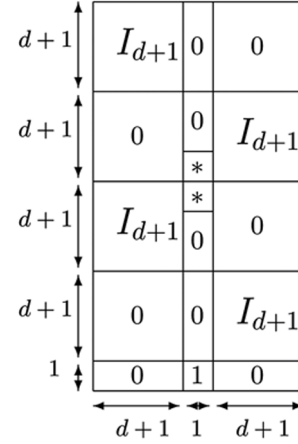
We start with the horizontal constraint. First, note that the i th row of T_n ($0 \leq i \leq 2n-3$) has the pattern

$$\begin{cases} 0^{n-i/2-2}10^{n+i/2+1}, & i \text{ even} \\ 0^{2n-\lfloor i/2 \rfloor -2}10^{\lfloor i/2 \rfloor +1}, & i \text{ odd.} \end{cases}$$

Hence, the i th row of the $[(4d+4) \times (2d+3), 2d+3]$ skeleton tile, $0 \leq i \leq 4d+3$, has the pattern

$$\begin{cases} 10^d 10^d 1, & i = 0 \\ 0^{d-(i-1)/2} 10^{d+(i-1)/2+2}, & i \text{ odd}, 1 \leq i \leq 2d \\ 0^{2d-\lfloor (i-1)/2 \rfloor +1} 10^{\lfloor (i-1)/2 \rfloor +1}, & i \text{ even}, 1 \leq i \leq 2d \\ 10^d * 0^d, & i = 2d+1 \\ 0^d * * 0^d, & i = 2d+2 \\ 0^d * 0^d 1, & i = 2d+3 \\ 0^{2d-i/2+1} 10^{i/2}, & i \text{ even}, 2d+4 \leq i < 4d+3 \\ 0^{3d-\lfloor i/2 \rfloor +2} 10^{\lfloor i/2 \rfloor -d-1}, & i \text{ odd}, 2d+4 < i \leq 4d+3. \end{cases}$$

Therefore, in the $[(4d+4) \times (2d+3), 2d+3]$ skeleton tile each row is a $(d, 2d+1)$ sequence. Now, consider the portions of the rows that cross two skeleton tiles. The scenario is depicted in Fig. 9. Now, one can easily verify that the constraint is not violated. Similar arguments hold for the columns. Hence, any standard tiling with \mathcal{A} and \mathcal{B} is a $(d, 2d+1, 2d, 2d+1)$ array. Therefore, by Lemma 3 $C_\diamond(d, 2d+1, 2d, 2d+1) > 0$. \square


 Fig. 10. A skeleton array for the $(d, 2d+2, 2d+1, 2d+2)$ constraint.

Lemma 5: $C_\diamond(d, 2d+2, 2d+1, 2d+2) > 0$ for every $d \geq 1$.

Proof: Consider the $(4d+5) \times (2d+3)$ skeleton array of Fig. 10. Let \mathcal{A} and \mathcal{B} be the two $(4d+5) \times (2d+3)$ arrays obtained from the skeleton array by substituting a *one* instead of one of the asterisks and a *zero* instead of the second asterisk. One can easily verify that any standard tiling with \mathcal{A} and \mathcal{B} yields a two-dimensional $(d, 2d+2, 2d+1, 2d+2)$ constrained array. Therefore, by Lemma 3 $C_\diamond(d, 2d+2, 2d+1, 2d+2) > 0$. \square

Lemma 6: If $d_1 \geq 1$, $k_1 > 2d_1$, $d_2 = k_1 - 1$, and $k_1 \leq k_2 \leq 2d_2$ then $C_\diamond(d_1, k_1, d_2, k_2) > 0$.

Proof: Assume $d_1 \geq 1$, $k_1 = 2d_1 + t$, $t > 0$, $d_2 = k_1 - 1$, and $k_2 = k_1$. We distinguish between two cases:

Case 1: $t = 2r + 1$, $r \geq 0$.

By Lemma 4, we have $C_\diamond(d_1 + r, 2d_1 + 2r + 1, 2d_1 + 2r, 2d_1 + 2r + 1) > 0$. Therefore, by Lemma 1, we have $C_\diamond(d_1, 2d_1 + 2r + 1, 2d_1 + 2r, 2d_1 + 2r + 1) > 0$.

Case 2: $t = 2r + 2$, $r \geq 0$.

By Lemma 5, we have $C_\diamond(d_1 + r, 2d_1 + 2r + 2, 2d_1 + 2r + 1, 2d_1 + 2r + 2) > 0$. Therefore, by Lemma 1 we have $C_\diamond(d_1, 2d_1 + 2r + 2, 2d_1 + 2r + 1, 2d_1 + 2r + 2) > 0$.

Hence, $C_\diamond(d_1, 2d_1 + t, 2d_1 + t - 1, 2d_1 + t) > 0$ and thus by Lemma 1 we have that if $d_1 \geq 1$, $k_1 > 2d_1$, $d_2 = k_1 - 1$, and $k_1 \leq k_2 \leq 2d_2$ then $C_\diamond(d_1, k_1, d_2, k_2) > 0$. \square

Lemma 7: If $d \geq 2$ and $d-1 \geq r \geq 1$ then $C_\diamond(d, 2d+1, d+r, d+r+1) > 0$.

Proof: We first define a $(d+r-1) \times d$ array $H_{d,r}$ recursively as follows. For $\rho \geq 1$, let

$$H_{\delta, 2\rho} = \begin{pmatrix} & & & 0 \\ & & & \vdots \\ & H_{\delta-1, 2\rho-1} & & \\ & & & 0 \\ 0 & \cdots & 0 & 0 \\ 0 & \cdots & 0 & 1 \end{pmatrix}$$

$$H_{\delta, 2\rho+1} = \begin{pmatrix} 1 & 0 & \cdots & 0 \\ 0 & 0 & \cdots & 0 \\ 0 & & & \\ \vdots & & & \\ 0 & & H_{\delta-1, 2\rho} & \end{pmatrix}$$

where $H_{\delta,1} = I_\delta$. $H_{8,6}$ is illustrated in Fig. 11.

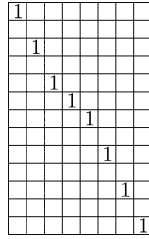


Fig. 11. The array $H_{8,6}$.

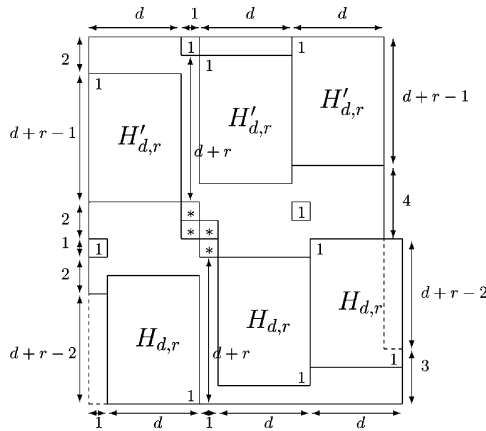


Fig. 12. The skeleton tile for $(d, 2d + 1, d + r, d + r + 1)$ constraint.

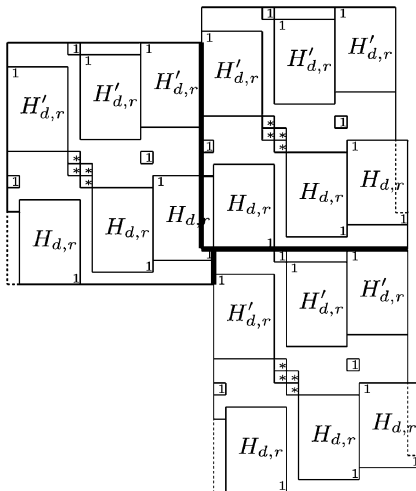


Fig. 13. Areas crossing two tiles for the $(d, 2d + 1, d + r, d + r + 1)$ constraint.

The $(d + r - 1) \times d$ array $H'_{d,r}$ is defined by the rotation of $H_{d,r}$ by 180° . Note that $H_{d,r} = H'_{d,r}$ if and only if r is odd. Also, in the “center” of $H_{d,r}$ ($H'_{d,r}$) there is the identity matrix I_{d-r+1} . This part of the array will be called *center*.

Consider the $[(2d + 2r + 4) \times (3d + 2), 2d + 2r + 1]$ skeleton tile of Fig. 12. Let \mathcal{A} and \mathcal{B} be the two $[(2d + 2r + 4) \times (3d + 2), 2d + 2r + 1]$ tiles obtained from the skeleton tile by substituting the two skew tetrominoes of Fig. 7 instead of the four asterisks.

As in the proof of Lemma 4, we have to prove that any standard tiling with \mathcal{A} and \mathcal{B} is a $(d, 2d + 1, d + r, d + r + 1)$ -constrained array. One can easily verify that it is sufficient to prove that the $[(2d + 2r + 4) \times$

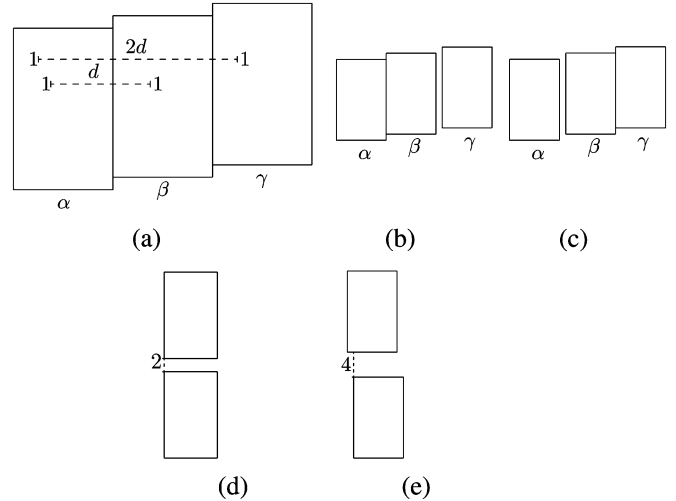


Fig. 14. Relative locations of $H_{d,r}$ arrays.

$(3d + 2), 2d + 2r + 1]$ skeleton tiles are $(d, 2d + 1, d + r, d + r + 1)$ tiles and that the constraint is not violated on rows and columns crossing two different skeleton tiles on the positions marked in bold in Fig. 8.

First note that rotating the plane by 180° , around any of the tetrominoes (while the tetrominoes are still labeled with the asterisks) leaves the plane with exactly the same labels. Note also that in Figs. 12 and 13 all the gaps between *ones*, in which at least one of the *ones* is not in $H_{d,r}$ or $H'_{d,r}$ are calculated and written. Therefore, we only have to calculate the gaps between *ones* in the rectangles depicted in Fig. 14. In each one of the three items (Fig. 14(a)–(c)), let α be the leftmost copy of $H_{d,r}$, β the middle copy, and γ the rightmost copy of $H_{d,r}$.

- 1) We start with the *ones* of Fig. 14(a). We calculate the gaps between *ones*, where one of the *ones* is in α . If the second *one* is in β then both *ones* belong to the center of $H_{d,r}$, and hence the gap between them is d . If the corresponding row in β consists only of *zeros*, then the corresponding row in γ contains a *one* as depicted in Fig. 14(a). The gap between these two *ones* is $2d$. The gaps between *ones* of β and γ are the same as the gaps between the *ones* of α and β .
- 2) The gaps between the *ones* of α and β in Fig. 14(b) are the same as the gaps between the *ones* of α and β in Fig. 14(a). The gaps between the *ones* of α and γ in Fig. 14(b), where the corresponding row of β has *zeros* are greater by one than the gaps between the *ones* of α and γ in Fig. 14(a), and hence, these gaps have length $2d + 1$. Similarly, the gaps between β and γ is $d + 1$.
- 3) The gaps between *ones* in Fig. 14(c), are handled similarly.
- 4) Since the height of $H_{d,r}$ is $d + r - 1$, it follows that the vertical gaps between *ones* in Fig. 14(d) are $d + r$ if r is odd. If r is even, then the gap between two *ones* is $d + r$ if at least one of them is not in the center of its shape, and $d + r + 1$ between the other *ones*.
- 5) The vertical gaps between *ones* in Fig. 14(e) are $d + r$ if r is even. If r is odd, then the gap between two *ones* is $d + r$ if at least one of them is not in the center of its shape, and $d + r + 1$ between the other *ones*.

Thus, any standard tiling with \mathcal{A} and \mathcal{B} is a $(d, 2d + 1, d + r, d + r + 1)$ constrained array. Therefore, by Lemma 3, $C_\diamond(d, 2d + 1, d + r, d + r + 1) > 0$. \square

Lemma 8: If $d_1 \geq 2, k_1 > 2d_1, d_1 < d_2 < k_1 - 1$, and $k_2 = d_2 + 1$, then $C_\diamond(d_1, k_1, d_2, k_2) > 0$.

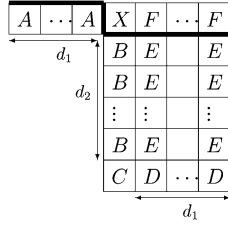


Fig. 15. Labels of the array in Proposition 1.

Proof: We distinguish between two cases:

- Case 1:** $d_1 < d_2 < 2d_1$.
By Lemma 7, we have $C_\diamond(d_1, 2d_1 + 1, d_2, d_2 + 1) > 0$ and hence, by Lemma 1, we have $C_\diamond(d_1, k_1, d_2, d_2 + 1) > 0$.
- Case 2:** $2d_1 \leq d_2 < k_1 - 1$.
By Lemma 6, we have $C_\diamond(d_1, d_2 + 1, d_2, d_2 + 1) > 0$ and hence, by Lemma 1, we have $C_\diamond(d_1, k_1, d_2, d_2 + 1) > 0$. □

Proposition 1: If $d_1 \geq 2, k_1 \leq 2d_1, d_1 \leq d_2 \leq k_1 - 1$, and $k_2 = d_2 + 1$, then $C_\diamond(d_1, k_1, d_2, k_2) = 0$.

Proof: Consider an array \mathcal{A} which is (d_1, k_1, d_2, k_2) constrained. We will show that the label X at position (i, j) is determined by the d_1 labels to the left of it, and the labels of the $(d_2 + 1) \times (d_1 + 1)$ array below it (see Fig. 15). Assume to the contrary that X can be labeled by a zero and can be labeled by a one. It implies that all the positions marked by A are zeros. If any of them is labeled with a one it would imply that X is a zero to avoid a pattern which violates the horizontal constraint. The same argument vertically implies that all the positions marked by B are zeros.

If the position marked by C is a zero then the positions marked by B or C form a run of k_2 zeros, which implies that X is a one. Hence, C is a one and all the positions marked by D are zeros to satisfy the horizontal constraint.

Consider the d_2 positions marked by E in one of the corresponding d_1 columns. If all these d_2 positions are zeros then the position marked by F in the same column should be labeled with a one by the vertical constraint and X is a zero by the horizontal constraint. Therefore, in each column with positions marked by E one of these positions is a one which implies that all the positions marked by F are labeled by zeros. Since all positions marked by A are also zeros, it follows that X is a one, which contradicts our assumption.

Thus, by Theorem 2 we have $C_\diamond(d_1, k_1, d_2, k_2) = 0$. □

The results in this section produce solutions to most of the seven unsolved cases. (u1) is solved in Lemma 4, (u2), (u3), and (u4) in Proposition 1, (u6) in Lemma 8, and (u7) in Lemma 6. (u5) was solved when $k_2 = d_2 + 1$ in Proposition 1. The only case which remained unsolved is $2 \leq d_1, d_1 + 2 \leq k_1 \leq 2d_1, d_2 = k_1 - 1$, and $d_2 + 2 \leq k_2 \leq 2d_2$.

IV. THE SQUARE MODEL

Let \mathcal{A} be an $n \times n$ array. We say that \mathcal{A} has n rows, n columns, n right diagonals, and n left diagonals. $A(i, j)$ belongs to row i , column j , right diagonal $[i - j]_n$, and left diagonal $[i + j]_n$, where $[\delta]_n$ is an integer σ such that $0 \leq \sigma \leq n - 1$ and $\delta \equiv \sigma \pmod{n}$. An $n \times n$ permutation array is a *doubly periodic nonattacking queens array* if each row, column, right diagonal, and left diagonal has exactly one one.

Lemma 9: A standard tiling with a $(d + 1) \times (d + 1)$ doubly periodic nonattacking queens array is a (d, d) array.

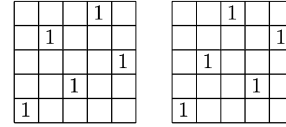


Fig. 16. Two 5×5 exchangeable arrays.

Proof: Let \mathcal{A} be a $(d + 1) \times (d + 1)$ doubly periodic nonattacking queens array. Consider the following $(2d + 2) \times (2d + 2)$ array:

$$\mathcal{B} = \begin{bmatrix} \mathcal{A} & \mathcal{A} \\ \mathcal{A} & \mathcal{A} \end{bmatrix}.$$

Clearly, each row (column) of \mathcal{B} has two ones separated by d zeros. Now, consider the bottom left and the upper right copies of \mathcal{A} . Each right diagonal which has a one on these arrays has two ones on the corresponding diagonal of \mathcal{B} . They are separated by d zeros as the other two copies of \mathcal{A} cannot have a one on the same right diagonal of \mathcal{B} . The same argument holds for the upper left and the lower right copies of \mathcal{A} , and the left diagonals.

Note, that any run of $d + 1$ symbols in the tiling has a representation in \mathcal{B} . Therefore, ones in each row of the tiling are separated by d zeros, and the same is true for columns, and diagonals. □

It is easy to verify that if \mathcal{A} is an infinite (d, d) array then any $(d + 1) \times (d + 1)$ subarray of \mathcal{A} is a doubly periodic nonattacking queens array. Thus, we have the following.

Corollary 1: An infinite (d, d) array exists if and only if a $(d + 1) \times (d + 1)$ doubly periodic nonattacking queens array exists.

If $A = (a_{ij})$ ($a_{ij} = A(i, j)$) is an $m \times m$ array and $B = (b_{rs})$ is an $n \times n$ array, then the direct product $A \times B$ is the $mn \times mn$ array given by

$$A \times B = \begin{bmatrix} a_{m1}B & a_{m2}B & \cdots & a_{mm}B \\ \vdots & \vdots & \cdots & \vdots \\ a_{21}B & a_{22}B & \cdots & a_{2m}B \\ a_{11}B & a_{12}B & \cdots & a_{1m}B \end{bmatrix}.$$

Note, that rows are ordered from bottom to top, which is some abuse of the traditional notation. A similar definition is given when A is an infinite array. One can easily verify the following.

Lemma 10: If \mathcal{A} is an $m \times m$ doubly periodic nonattacking queens array and \mathcal{B} is an $n \times n$ doubly periodic nonattacking queens array, then $\mathcal{A} \times \mathcal{B}$ is a doubly periodic $mn \times mn$ nonattacking queens array.

Let \mathcal{P} and \mathcal{Q} be the two 5×5 doubly periodic nonattacking queens arrays given in Fig. 16. The ones in both arrays occupy the same rows, columns, and diagonals (without considering them periodic modulo 5). Therefore, we have the following statement.

Lemma 11: If \mathcal{A} is an infinite (d, d) array then any exchanges of copies of \mathcal{P} with copies of \mathcal{Q} in disjoint positions of \mathcal{A} will result in a $(d - 3, d + 3)$ array.

For $r \not\equiv 2 \pmod{3}$ let

$$\mathcal{L}_r = \{(x, y) : x = 2j + \ell, y = j + r\ell, j, \ell \in \mathcal{Z}\} \quad (1)$$

be a set of lattice points in \mathbb{Z}^2 .

Lemma 12: If $(x, y) \in \mathcal{L}_r$ then

- $(x - 2r + 1, y + 2r - 1), (x, y + 2r - 1), (x + 2r - 1, y + 2r - 1), (x + 2r - 1, y) \in \mathcal{L}_r$;

- $(x - j, y + j), (x, y + j), (x + j, y + j), (x + j, y) \notin \mathcal{L}_r$, for all $j, 1 \leq j \leq 2r - 2$.

Proof: Assume $(x, y) \in \mathcal{L}_r$ for some $r \in \mathbb{Z}$. To prove the lemma we have to solve each one of the four sets of equations:

- 1) $x + 2j + l = x - s$ and $y + j + rl = y + s$,
- 2) $x + 2j + l = x$ and $y + j + rl = y + s$,
- 3) $x + 2j + l = x + s$ and $y + j + rl = y + s$,
- 4) $x + 2j + l = x + s$ and $y + j + rl = y$,

where $0 < s < 2r$ in all the four sets of equations. The solutions correspond to the two claims of the lemma. It is elementary algebra to verify the solutions of these sets. \square

Corollary 2: Let $d = 2r$, $r \not\equiv 1 \pmod{3}$ be an even integer and let \mathcal{A} be an infinite array, where $\mathcal{A}(i, j) = 1$ if $(i, j) \in \mathcal{L}_{r+1}$. Then \mathcal{A} is a (d, d) array.

By Corollary 1 and Lemma 10 we have the following.

Lemma 13: If \mathcal{A} is a (d, d) array then $\mathcal{A} \times \mathcal{P}$ is a $(5d + 4, 5d + 4)$ array.

From Lemmas 3, 11, 13, and Corollary 2 we have the following.

Theorem 3: $C_{\boxplus}(d, d + 6) > 0$, $d \equiv 1, 21 \pmod{30}$.

Instead of the 5×5 arrays \mathcal{P} and \mathcal{Q} we can take other $n \times n$ arrays, when $n \equiv 1$ or $5 \pmod{6}$. Let \mathcal{P}_n be the array defined by $\mathcal{P}_n(i, j) = 1$ iff $j \equiv 2i \pmod{n}$ and let \mathcal{Q}_n be the array defined by $\mathcal{Q}_n(i, j) = 1$ iff $i \equiv 2j \pmod{n}$. Note, that \mathcal{P}_5 and \mathcal{Q}_5 are \mathcal{P} and \mathcal{Q} . It is also easy to verify the following.

Lemma 14: \mathcal{Q}_n is a subarray of $\mathcal{L}_{\frac{n+1}{2}}$.

Lemma 15: If \mathcal{A} is an infinite (d, d) array then any exchanges of copies of \mathcal{P}_n with copies of \mathcal{Q}_n in disjoint positions of \mathcal{A} will result in a $(d - n + 3, d + n - 3)$ array if $n \geq 7$.

Proof: By definition \mathcal{Q}_n and \mathcal{P}_n have mirror symmetry around the line $y = x$. Moreover, since

$$\{i - j : \mathcal{P}_n(i, j) = 1\} = \{i - j : \mathcal{Q}_n(i, j) = 1\}$$

it follows that the *ones* in both arrays occupy the same rows, columns, and diagonals (without considering them periodic modulo n).

For $n \geq 7$, the line in which the difference between *ones* of \mathcal{P}_n and \mathcal{Q}_n is the largest, is the one in which $\mathcal{P}_n(n - 1, n - 2) = 1$ and $\mathcal{Q}_n(2, 1) = 1$. The gap between these two positions is $n - 3$ and hence any exchanges of copies of \mathcal{P}_n with copies of \mathcal{Q}_n in disjoint positions of \mathcal{A} will result in a $(d - n + 3, d + n - 3)$ array. \square

Note that Lemma 15 does not hold for $n = 5$.

Now, by applying Lemma 10 on $\mathcal{L}_{\frac{d+1}{2}}$ and \mathcal{P}_n we obtain an $(n(d + 1) - 1, n(d + 1) - 1)$ array \mathcal{A} . By exchanging copies of \mathcal{P}_n with copies of \mathcal{Q}_n in disjoint positions of \mathcal{A} we obtain an $(nd + 2, n(d + 2) - 4)$ array and hence, by Lemma 3, we have the following.

Theorem 4: $C_{\boxplus}(nd + 2, n(d + 2) - 4) > 0$, for odd $n \not\equiv 3 \pmod{6}$, $n \geq 7$, and even $d \not\equiv 2 \pmod{6}$.

Corollary 3:

- $C_{\boxplus}(d, d + 8) > 0$, $d \equiv 2$ or $30 \pmod{42}$.
- $C_{\boxplus}(d, d + 16) > 0$, $d \equiv 2$ or $46 \pmod{66}$.

Each one of the values $C_{\boxplus}(44, 52) > 0$, $C_{\boxplus}(72, 80) > 0$, $C_{\boxplus}(244, 260) > 0$, and $C_{\boxplus}(266, 282) > 0$ is obtained only by one of the four cases in Corollary 3 and cannot be handled by Theorem 3. For $n = 13$, we consider two different permutation arrays \mathcal{P}' and \mathcal{Q}' . Let \mathcal{P}' be the array defined by $\mathcal{P}'(i, j) = 1$ iff $j \equiv 3i \pmod{n}$ and \mathcal{Q}' be the array defined by $\mathcal{Q}'(i, j) = 1$ iff $i \equiv 3j \pmod{n}$. Similarly to Corollary 3 we have the following.

Theorem 5: $C_{\boxplus}(d, d + 18) > 0$, $d \equiv 3$, or $55 \pmod{78}$. The values $C_{\boxplus}(367, 385) > 0$ and $C_{\boxplus}(393, 411) > 0$ are obtained from Theorem 5 and cannot be obtained from Theorem 3 and Corollary 3. For small values of d , the zero/positive capacity region is slightly different. For example, by using a $(4, 4)$ array and replacing any set of *ones*, in which no two *ones* have a gap of length 4, with *zeros*, we prove that $C_{\boxplus}(4, 9) > 0$.

Theorem 6: If n is even then there is no $n \times n$ doubly periodic nonattacking queens array.

Proof: Assume that n is even and an $n \times n$ doubly periodic nonattacking queens array \mathcal{A} exists. We write \mathcal{A} as a sequence a_0, a_1, \dots, a_{n-1} , where $a_j = i$ if and only if $\mathcal{A}(i, j) = 1$. Since \mathcal{A} is a doubly periodic nonattacking queens array, it follows that $[a_0]_n, [a_1 - 1]_n, \dots, [a_{n-1} - (n - 1)]_n$, is a permutation of $0, 1, \dots, n - 1$. For any given permutation p_0, p_1, \dots, p_{n-1} of $0, 1, \dots, n - 1$ we have

$$\sum_{i=0}^{n-1} p_i = \frac{(n-1)n}{2} \equiv \frac{n}{2} \pmod{n} \quad (2)$$

since n is even. Therefore,

$$\sum_{i=0}^{n-1} (a_i - i) = \sum_{i=0}^{n-1} a_i - \sum_{i=0}^{n-1} i \equiv 0 \pmod{n}.$$

Hence, by (2) again $[a_0]_n, [a_1 - 1]_n, \dots, [a_{n-1} - (n - 1)]_n$ cannot be a permutation, a contradiction.

Thus, if n is even, then there is no $n \times n$ doubly periodic nonattacking queens array. \square

Theorem 7: If $n \equiv 0 \pmod{3}$ and there exists an $n \times n$ doubly periodic nonattacking queens array then $n \equiv 0 \pmod{9}$.

Proof: Assume that $n \equiv 0, 3$, or $6 \pmod{9}$ and an $n \times n$ doubly periodic nonattacking queens array \mathcal{A} exists. We write \mathcal{A} as a sequence a_0, a_1, \dots, a_{n-1} , where $a_j = i$ if and only if $\mathcal{A}(i, j) = 1$. Since \mathcal{A} is a doubly periodic nonattacking queens matrix, it follows that

$$[a_0]_n, [a_1 - 1]_n, \dots, [a_{n-1} - (n - 1)]_n$$

and

$$[a_0]_n, [a_1 + 1]_n, \dots, [a_{n-1} + n - 1]_n$$

are permutations of $0, 1, \dots, n - 1$. Let $p_i = [a_i - i]_n$, $0 \leq i \leq n - 1$. p_0, p_1, \dots, p_{n-1} is a permutation of $0, 1, \dots, n - 1$ such that

$$[p_0]_n, [p_1 + 1]_n, \dots, [p_{n-1} + n - 1]_n$$

and

$$[p_0]_n, [p_1 + 2]_n, \dots, [p_{n-1} + 2(n - 1)]_n$$

are also permutations of $0, 1, \dots, n - 1$. Let

- $t = |\{i : i \equiv 0 \pmod{3} \text{ and } p_i \equiv 0 \pmod{3}\}|$
- $s = |\{i : i \not\equiv 0 \pmod{3} \text{ and } p_i \not\equiv 0 \pmod{3}\}|$.

Given an integer $\nu \not\equiv 0 \pmod{3}$ such that $p_\nu \not\equiv 0 \pmod{3}$ we have that either $p_\nu + 1$ or $p_\nu + 2$ is congruent to 0 modulo 3, and since $|\{i : p_i + i \equiv 0 \pmod{3}\}| = |\{i : p_i + 2i \equiv 0 \pmod{3}\}| = \frac{n}{3}$ we have

$$t + \frac{s}{2} = \frac{n}{3}. \quad (3)$$

A	...	A	X	Y ₁	Y ₂	Y ₃	

 Fig. 17. Scanning of a $(d, d + 3)$ array.

				B	E	E	B			
					D	C				
				C	E	E	D			
A	...	A	X	B	B	Y ₃				
			B	B	E ^d	E	B	B		
					⋮	⋮				
	...		d	⋮	E	E	⋮		...	
					F	F				
B				B	F	F	B			B

Fig. 18. Case 1 in the proof of Theorem 8.

Clearly, $|\{i : i \not\equiv 0 \pmod{3} \text{ and } p_i \equiv 0 \pmod{3}\}|$ is equal to $\frac{n}{3} - t$ and also to $2\frac{n}{3} - s$ and hence,

$$\frac{n}{3} - t = 2\frac{n}{3} - s. \quad (4)$$

By solving (3) and (4) we have that $t = \frac{n}{9}$. \square

Theorem 8: $C_{\boxplus}(d, d + 3) = 0$ for every $d \geq 1$.

Proof: If $d \in \{1, 2\}$, then the theorem can be easily verified (see [3]). If $d \in \{3, 4, 5\}$, then the theorem follows from Theorem 9 in Section V which follows.

Assume $d \geq 6$, and consider an array \mathcal{A} which is $(d, d + 3)$ constrained. We will show that the label X at position (i, j) is determined by the labels to the left of it and labels below it (see Fig. 17).

Assume to the contrary that X can be labeled by a zero and can be labeled by a one. It implies that all the positions marked by A are zeros and either X or one of the three positions to right of X is a one. Therefore, at least one of the following three cases must be valid.

Case 1: X can be a one and Y_3 can be a one (see Fig. 18).

Clearly, all positions marked by B are zeros. Therefore, if X is a zero then by the vertical constraint and the right diagonal constraint, the positions marked by C will be labeled by ones. Similarly, if Y_3 is a zero then by the vertical constraint and the left diagonal constraint, the positions marked by D will be labeled by ones. This implies that all positions marked by E must be zeros. Hence, to avoid a vertical run of $d + 4$ zeros two of the four positions marked by F must be ones, which is clearly impossible.

Case 2: X can be a one and Y_2 can be a one (see Fig. 19).

As in Case 1, the positions marked by B are zeros. Also, if X is a zero then the positions marked by C_1 and C_2 will be labeled by ones, and if Y_2 is a zero then the positions marked by D will be labeled by ones. Therefore, the positions marked by E must be zeros, which implies, by the diagonals constraints, that if C_2 is a zero then both F_1 and F_2 will be ones, a contradiction to the horizontal constraint.

Case 3: X can be a one and Y_1 can be a one.

This case is verified easily and the contradiction is similar to the one in Case 1.

Thus, $C_{\boxplus}(d, d + 3) = 0$. \square

					F ₂					F ₁
				E	D	E	E	E	C ₁	
				E	B	E	B			
						C ₂	B	D		
A	...			A	X	B	Y ₂			
				E	B	B	B	B		
				B	B	B	E	B		
	
		...		d	⋮	⋮		
E										E
B					B	B				B

Fig. 19. Case 2 in the proof of Theorem 8.

	1	
		1
1		

		1
1		
	1	

 Fig. 20. Two 3×3 exchangeable arrays.

V. THE HEXAGONAL MODEL

Kukorely and Zeger [12], [13] have found some of the positive capacity region for two-dimensional constrained channels in the hexagonal model. Their results are summarized in the following theorem.

Theorem 9:

- If $d \equiv 0 \pmod{6}$ then $C_{\square}(d, d + 4) > 0$.
- If $d \geq 2$ is even then $C_{\square}(d, 2d + 1) > 0$.
- $C_{\square}(d, d + 2) = 0$ for every $d \geq 1$.
- If $d \in \{3, 4, 5, 7, 9, 11\}$ then $C_{\square}(d, d + 3) = 0$.

In the hexagonal model there are three directions: horizontal (rows), vertical (columns), and diagonal (right diagonals). An $n \times n$ permutation array is a *doubly periodic nonattacking semi-queens array* if each row, each column, and each right diagonal has exactly one one.

Similarly to Lemma 9, we have the following.

Lemma 16: A standard tiling with a doubly periodic $(d + 1) \times (d + 1)$ nonattacking semi-queens array is a (d, d) array.

The proof of Theorem 6 also implies the following result.

Theorem 10: If n is even then there is no $n \times n$ doubly periodic nonattacking semi-queens array.

For even $n \geq 6$, $(n + 3) \times (n + 3)$ doubly periodic nonattacking semi-queens arrays exist for all n 's. We will use the following $n \times n$ skeleton array:

$$\mathcal{B} = \begin{bmatrix} \mathbf{0} & \mathcal{P} \\ H_n & \mathbf{0} \end{bmatrix}$$

where H_n is an appropriate $n \times n$ permutation array, and \mathcal{P} is a 3×3 array. Let \mathcal{A}_{n+3} and \mathcal{B}_{n+3} be the two $(n + 3) \times (n + 3)$ arrays obtained from the skeleton array by substituting in \mathcal{P} the two 3×3 arrays shown in Fig. 20. If \mathcal{A}_{n+3} and \mathcal{B}_{n+3} are $(n + 3) \times (n + 3)$ doubly periodic nonattacking semi-queens arrays then by similar arguments to those used in Section IV and Lemma 3, we will have that $C_{\square}(n, n + 4) > 0$.

In the construction of H_n we distinguish between the even values of n modulo 10. Each such value has a different construction. The first arrays in each congruence modulo 10 are presented in Figs. 21 and 22. The generalization is readily verified and the proofs that the arrays have the required properties are easy to observe and hence they

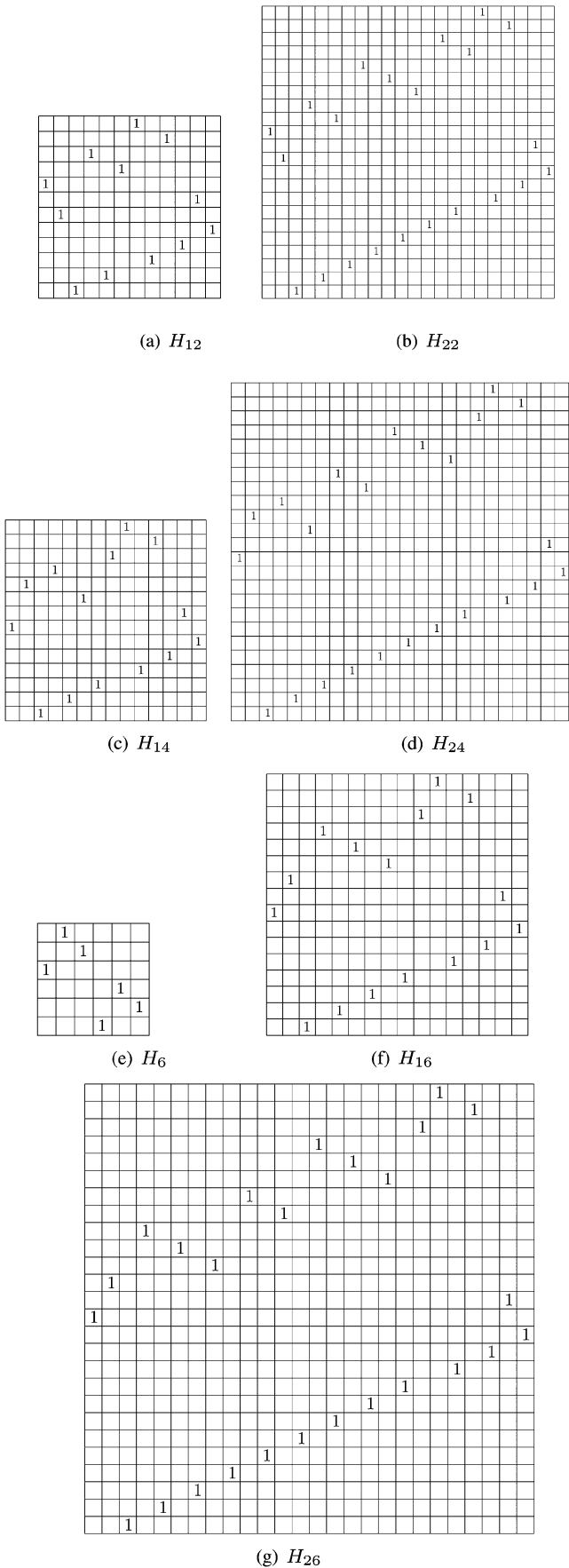


Fig. 21. Some arrays H_n , for $n \equiv 2, 4, 6 \pmod{10}$.

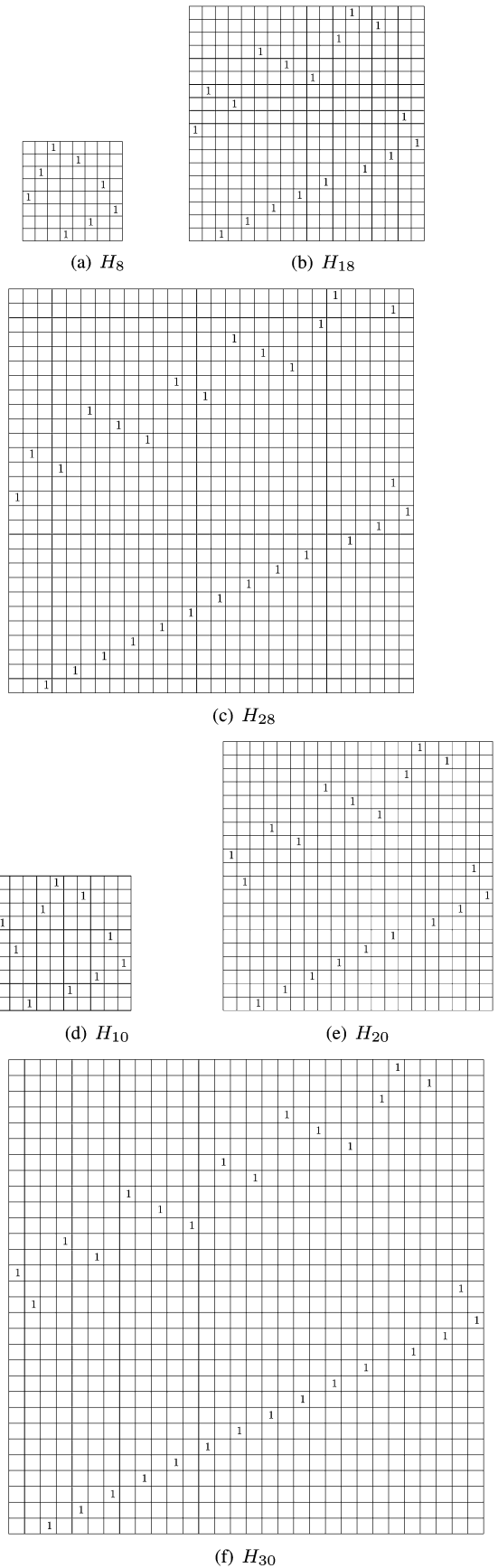


Fig. 22. Some arrays H_n , for $n \equiv 8, 0 \pmod{10}$.

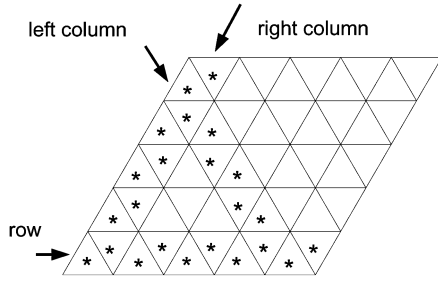


Fig. 23. A triangular array.

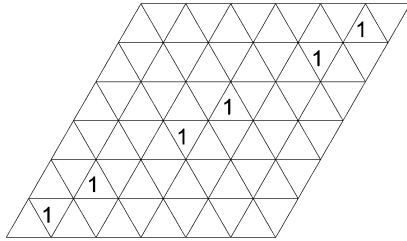


Fig. 24. The triangular array T_6 .

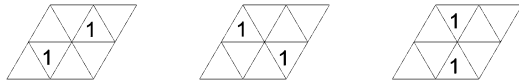


Fig. 25. Three 2×2 exchangeable triangular arrays.

will be omitted and left for the reader. Hence, we have the following theorem.

Theorem 11: $C_{\square}(d, d + 4) > 0$, for even $d > 5$.

VI. THE TRIANGULAR MODEL

Let \mathcal{A} be an $n \times n$ triangular array. We say that \mathcal{A} has n rows, n right columns, and n left columns. $A(i, j, s)$ belongs to row i , right column j , left column $[i + j + s]_n$ (see Fig. 23). An $n \times n$ triangular array is called a *doubly periodic nonattacking triangle queens array* if each row, right column, and left column has exactly one *one*. The following two lemmas are proved similarly to Lemmas 9 and 11.

Lemma 17: An $n \times n$ doubly periodic nonattacking triangle queens array exists if and only if a $(2n - 1, 2n - 1)$ triangular array exists.

Lemma 18: If \mathcal{A} is an $n \times n$ (d, d) triangular array then any exchanges of copies of the patterns shown in Fig. 25 in disjoint positions of \mathcal{A} will result in a $(d - 2, d + 2)$ array.

Lemma 19: If $d \equiv 1 \pmod{4}$ then

$$C_{\Delta}(d, d + 4) \geq \frac{1}{2(d + 3)} \log_2 3.$$

Proof: For n even, we construct the following $n \times n$ doubly periodic nonattacking triangle queens array T_n , where $T_n(i, i, s) = 1$ if $s \neq i \pmod{2}$, $0 \leq i \leq n - 1$ (T_6 is illustrated in Fig. 24). By Lemma 17, the standard tiling with T_n is a $(2n - 1, 2n - 1)$ array. By Lemma 18, any exchanges of copies of the pattern shown in Fig. 25 in disjoint positions of \mathcal{A} will result in a $(2n - 3, 2n + 1)$ array. The total number of different $(2n - 3, 2n + 1)$ arrays used in the tiling is $3^{\frac{n}{2}}$. Hence, by Lemma 3 we have that $C_{\Delta}(2n - 3, 2n + 1) \geq \frac{1}{4n} \log_2 3$. \square

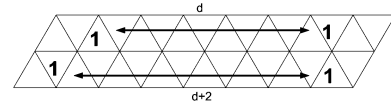


Fig. 26. The pattern PEven.

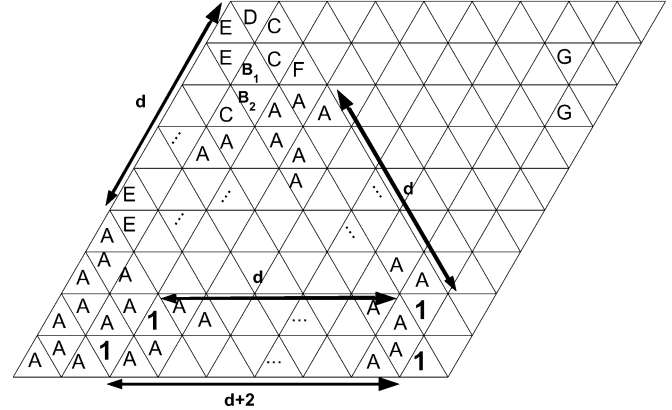


Fig. 27. Labels implied by the pattern PEven.

Lemma 20: If n is odd then there is no $n \times n$ doubly periodic nonattacking triangle queens array which contains an appearance of one of the patterns shown in Fig. 25.

Proof: Assume that n is odd and an $n \times n$ doubly periodic nonattacking triangle queens array \mathcal{A} exists. We write \mathcal{A} as a sequence a_0, a_1, \dots, a_{n-1} , where $a_i = (j_i, s_i)$ if $\mathcal{A}(i, j_i, s_i) = 1$. Since \mathcal{A} is a doubly periodic nonattacking triangle queens array, it follows that for $0 \leq r < \ell \leq n - 1$ we have $j_r \neq j_\ell$ and

$$j_r + r + s_r \not\equiv j_\ell + \ell + s_\ell \pmod{n}.$$

Therefore, j_0, j_1, \dots, j_{n-1} and

$$[j_0 + 0 + s_0]_n, [j_1 + 1 + s_1]_n, \dots, [j_{n-1} + (n - 1) + s_{n-1}]_n$$

are permutations of $0, 1, \dots, n - 1$. For any given permutation p_0, p_1, \dots, p_{n-1} of $0, 1, \dots, n - 1$ we have

$$\sum_{i=0}^{n-1} p_i = \frac{(n - 1)n}{2} \equiv 0 \pmod{n} \tag{5}$$

since n is odd. Therefore,

$$\sum_{i=0}^{n-1} s_i = \sum_{i=0}^{n-1} (j_i + i + s_i) - \sum_{i=0}^{n-1} j_i - \sum_{i=0}^{n-1} i \equiv 0 \pmod{n}.$$

Hence, for each $0 \leq r < \ell \leq n - 1$, we have $s_r = s_\ell$. Thus, there is no doubly periodic $n \times n$ nonattacking triangle queens array which contains an appearance of any 2×2 array shown in Fig. 25. \square

Lemma 21: Let $d \geq 6$ be an even integer, $h = \frac{d+6}{2}$, and let \mathcal{A} be an infinite $(d, d + 3)$ array. If \mathcal{A} contains an $r \times h$ subarray \mathcal{B} whose first two rows form the pattern PEven (see Fig. 26), then the first two and the last two right columns of \mathcal{B} are substrings of $(10^{d+1})^\infty$.

Proof: Let \mathcal{C} be an $r \times (h + 1)$ sub-array of \mathcal{A} with the pattern PEven as depicted in Fig. 27. Clearly, the positions marked by A are zeros. By the left column constraint either B_1 or B_2 will be a *one* and hence all positions marked by C are zeros. Assume the position marked by D is a *one*. Then, all positions marked by E will be zeros which will

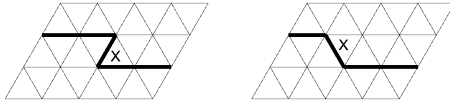


Fig. 28. The possible orientations of a scanned position.

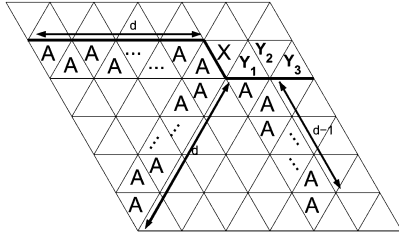


Fig. 29. Case 1 of Lemma 22.

create a run-length of $d + 7$ zeros in the right column, a contradiction. Hence, D is a zero, F is a one, B_1 is a zero, and B_2 is a one.

The four ones in the left columns of B_2 and F form the pattern PEven and hence by the same arguments the two positions marked by G are ones. The positions marked by B_2 , F , and G form again the pattern PEven. The claim of the lemma is proved now by induction. \square

Lemma 22: If $d \geq 6$ is even then $C_{\Delta}(d, d + 3) = 0$.

Proof: We will use the scanning technique again. Assume we have to label the next scanned position marked by X . We have to distinguish between two different types of orientations of the position as depicted in Fig. 28.

Case 1: Assume that X , as depicted in Fig. 29 (to simplify the picture, the array is drawn in a different orientation), is not uniquely determined, i.e., it can be labeled by a zero and it can be labeled by a one. It implies that all the positions marked by A are zeros, either X or one of the three positions to right of X is a one, and at least one of the following three cases must be valid.

Case 1a: X can be a one and Y_1 can be a one. Clearly, all positions marked by B are zeros (see Fig. 30). X can be a zero and hence, either C_1 or C_2 is a one. Y_1 can be a zero and therefore either D_1 or D_2 is a one. It implies that C_1 and D_1 are ones. Hence, all positions marked by E are zeros. By the horizontal constraint either F_1 or F_2 is a one. Since Y_1 can be a zero, it follows that either G_1 or G_2 is a one. Hence, F_1 is a one and all positions marked by H are zeros.

Assume I will be a one. Then all positions marked by J will be zeros, creating a run with $d + 4$ zeros in their right column, a contradiction. Therefore, I is labeled by a zero.

Assume all the $d - 5$ positions marked by K are zeros. Then L_1 is labeled by a one and Y_1 cannot be a one, a contradiction. Hence, one of the positions marked by K is a one, L_1 and L_2 are labeled by zeros.

Therefore, if X will be a one then Y_1 will be a zero and by its right column constraint M will be a one. M , X , C_1 , and D_1 will form the pattern PEven, and hence, by Lemma 21, the whole prefix of the row before X is a given sequence $\mathcal{P}(i, j)$, and we are in state (s3).

Case 1b: X can be a one and Y_2 can be a one. Clearly, all positions marked by B are zeros (see Fig. 31). X can be a zero, and hence exactly one of the C_i 's is a one, and exactly one of the D_i 's is a one. Y_2 can be a zero and therefore exactly one of the E_i 's is a one, and exactly one of the F_i 's is a one. Clearly, D_3 and E_3 cannot be ones.

- If E_2 is a one then C_1 is a one. If X will be a one then Y_2 will be a zero and by its left column constraint G will be a one. E_2 , C_1 , X , and G will form the pattern PEven, and hence, by Lemma 21, the whole prefix of the row before X is a given sequence $\mathcal{P}(i, j)$, and we are in state (s3).
- If D_2 is a one then F_1 is a one. If Y_2 will be a one then X will be a zero and by its right column constraint H will be a one. D_2 , F_1 ,

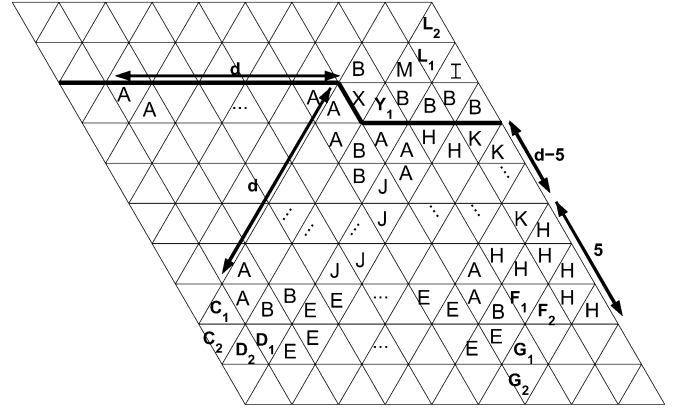


Fig. 30. Case 1a of Lemma 22.

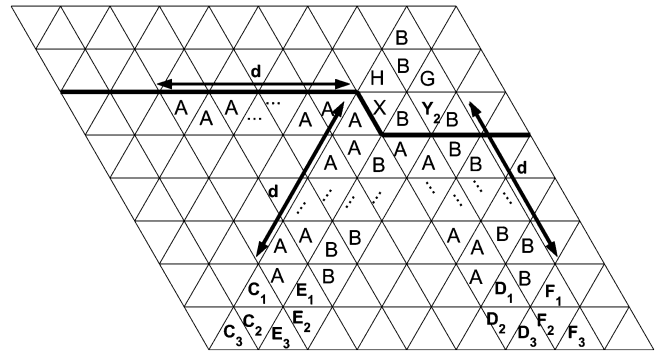


Fig. 31. Case 1b of Lemma 22.

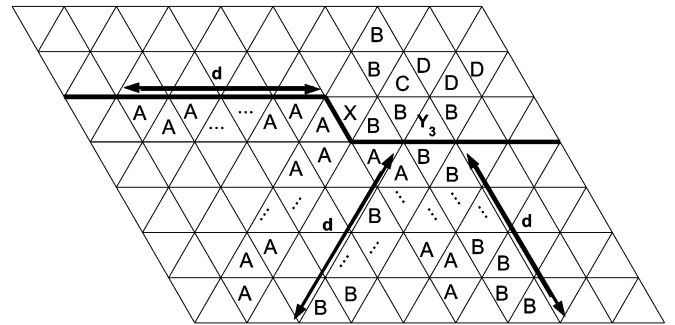


Fig. 32. Case 1c of Lemma 22.

Y_2 , and H will form the pattern PEven, and hence, by Lemma 21, the suffix of the current row is completely determined, and we are in state (s2).

- If D_2 , D_3 , E_2 , and E_3 are zeros then D_1 and E_1 are ones which is impossible since the gap between them is $d - 1$ and the run-length constraint will be violated.

Case 1c: X can be a one and Y_3 can be a one. Clearly, all positions marked by B are zeros (see Fig. 32). If X will be a one then Y_3 will be a zero and by its left column constraint C will be a one. Hence, all the positions marked by D will be labeled by zeros, creating a run of $d + 4$ zeros in the right column of Y_3 , a contradiction.

Case 2: If X is a position in the second orientation we proceed similarly to Case 1. The proof is similar, easier, and shorter. It can be found in [3]. \square

Lemma 23: Let $d \geq 5$ be an odd integer, $h = \frac{d+7}{2}$, and let \mathcal{A} be an infinite $(d, d + 3)$ array. If \mathcal{A} contains an $r \times h$ subarray \mathcal{B} whose first

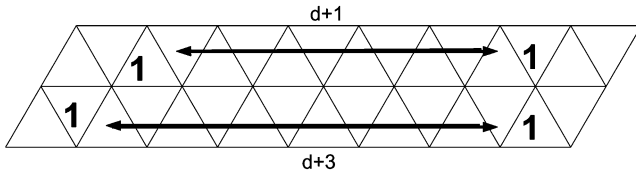


Fig. 33. The pattern POdd.

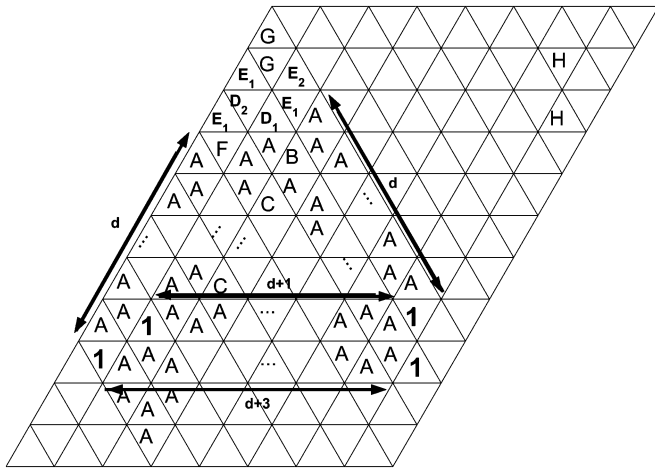


Fig. 34. Labels implied by the pattern POdd.

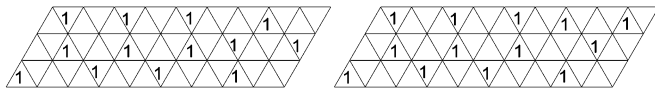


Fig. 35. Two triangular arrays to prove that $C_\Delta(2, 4) > 0$.

two rows form the pattern POdd (see Fig. 33), then the first two and the last two right columns of \mathcal{B} are substrings of $(10^{d+2})^\infty$.

Proof: Let \mathcal{C} be an $(r + 2) \times h$ right subarray of \mathcal{A} with the pattern POdd as depicted in Fig. 34. Clearly the positions marked by A are zeros.

Assume the position marked by B is a one. Then the $d - 4$ positions marked by C will be zeros, creating a run of $d + 4$ zeros in their right column, a contradiction. Therefore, B is a zero and either D_1 or D_2 is a one.

Assume D_1 is a one. Then D_2 and all positions marked by E_1 or E_2 will be zeros. Hence, F will be a one and the two positions marked by G will be zeros, and it will create a run-length of $d + 4$ zeros in their left column, a contradiction. Therefore, D_1 is a zero and D_2 is a one. It implies that all positions marked by E_1 or G are zeros, and hence E_2 is a one.

The four ones in the left columns of D_2 and E_2 form the pattern POdd and hence by the same arguments the two positions marked by H are ones. The positions marked by D_2 , E_2 , and H form again the pattern POdd. The claim of the lemma is proved now by induction. \square

Similarly to Lemma 24, we have the following lemma that has a similar shorter proof which can be found in [3].

Lemma 24: If $d \geq 5$ is odd then $C_\Delta(d, d + 3) = 0$.

Corollary 4: $c_\Delta(d, d + 3) = 0$ for $d \geq 5$.

For small values of d , the zero/positive capacity region is slightly different. For example, it is a simple exercise to prove that $C_\Delta(1, 3) > 0$, $C_\Delta(3, 7) > 0$ by using $(1, 1)$ and $(3, 3)$ arrays, respectively. A tiling with the lattice points $\{(x, y) : x = 3i, y = 3i + 9j, i, j \in \mathbb{Z}\}$

and the two triangular arrays of Fig. 35 imply that $C_\Delta(2, 4) > 0$. By using case analysis similarly to the one used in Lemma 22 we can prove that $C_\Delta(3, 6) = 0$. By Lemma 24, we have that $C_\Delta(5, 8) = 0$ and hence if a $(4, 8)$ array exists then there exists a run of zeros whose length is exactly 4. Starting with this and analyzing the array one can easily obtain that a run of zeros whose length is 9 must exist. Hence, $C_\Delta(4, 8) = 0$. The complete proofs appear in [3].

VII. DISCUSSION AND OPEN PROBLEMS

We considered the positive capacity region of two-dimensional run-length-constrained channels in four connectivity models—the diamond, square, hexagonal, and triangular models. We have managed to find some regions where the capacity is positive and some in which the capacity is zero, by using generalizations and modifications of known techniques. Some regions remain open for future research. The following problems should be the focus of further research.

- 1) The scanning method of [2] was generalized in Theorem 2. Can it further be generalized to handle constraints in which the number of constrained arrays is much larger?
- 2) For $2 \leq d_1, d_1 + 2 \leq k_1 \leq 2d_1, d_2 = k_1 - 1, d_2 + 2 \leq k_2 \leq 2d_2$, is $C_\diamond(d_1, k_1, d_2, k_2) = 0$ or $C_\diamond(d_1, k_1, d_2, k_2) > 0$? This is the only unknown value for asymmetric constraints in the diamond model.
- 3) When $n \equiv 0 \pmod{9}$, is there a permutation p_0, p_1, \dots, p_{n-1} of $0, 1, \dots, n - 1$ such that

$$[p_0]_n, [p_1 + 1]_n, \dots, [p_{n-1} + n - 1]_n$$

and

$$[p_0]_n, [p_1 + 2]_n, \dots, [p_{n-1} + 2(n - 1)]_n$$

are also permutations of $0, 1, \dots, n - 1$?

- 4) Find an infinite set S of positive integers and an integer r such that $C_\square(d, d + r) = 0$ and $C_\square(d, d + r + 1) > 0$ for each $d \in S$. The same problem should be considered for the square model.
- 5) How good is the bound on the capacity given in Lemma 3? For example, can the bound of Lemma 19

$$C_\Delta(d, d + 4) \geq \frac{1}{2(d + 3)} \log_2 3, \quad \text{for } d \equiv 1 \pmod{4}$$

be improved?

Finally, some of the results we gave can be readily generalized. For example, Lemma 11 can be generalized as follows.

Lemma 25: Let \mathcal{A} be an infinite (d, k) array in the square model. Then, any exchanges of copies of \mathcal{P} with copies of \mathcal{Q} , in disjoint positions of \mathcal{A} which do not share a run of zeros, will result in a $(d - 3, k + 3)$ array.

Similar generalizations exist for the hexagonal and the triangular models.

ACKNOWLEDGMENT

The authors wish to thank Ken Zeger for providing his results and Simon Blackburn for providing [2].

REFERENCES

- [1] J. J. Ashley and B. H. Marcus, "Two-dimensional low-pass filtering codes," *IEEE Trans. Commun.*, vol. 46, no. 6, pp. 724–727, Jun. 1998.
- [2] S. R. Blackburn, "Two dimensional runlength constrained arrays with equal horizontal and vertical constraints," *IEEE Trans. Inf. Theory*, to be published.
- [3] K. Censor, "Constrained Codes for Two-Dimensional Channels," M.Sc. thesis, Computer Science Department, Technion–Israel Inst. Technol., Haifa, Israel, 2006.
- [4] J. H. Conway and N. J. A. Sloane, *Sphere Packings, Lattices, and Groups*. New York: Springer-Verlag, 1988.

- [5] S. I. Costa, M. Muniz, E. Agustini, and R. Palazzo, "Graphs, tessellations, and perfect codes on flat tori," *IEEE Trans. Inf. Theory*, vol. 50, no. 10, pp. 2363–2377, Oct. 2004.
- [6] T. Etzion and K. Paterson, "Zero/positive capacities two-dimensional runlength-constrained arrays," *IEEE Trans. Inf. Theory*, vol. 51, no. 9, pp. 3186–3199, Sep. 2005.
- [7] T. Etzion and A. Vardy, "Two-dimensional interleaving schemes with repetitions: Constructions and bounds," *IEEE Trans. Inf. Theory*, vol. 48, no. 11, pp. 428–457, Nov. 2002.
- [8] K. A. S. Immink, *Coding Techniques for Digital Recorders*. New York: Prentice-Hall, 1991.
- [9] —, *Codes for Mass Data Storage Systems*. Amsterdam, The Netherlands: Shannon Foundation Publishers, 1999.
- [10] A. Kato and K. Zeger, "On the capacity of two-dimensional run length constrained channels," *IEEE Trans. Inf. Theory*, vol. 45, no. 5, pp. 1527–1540, Jul. 1999.
- [11] —, "Partial characterization of the positive capacity region of two-dimensional asymmetric run length constrained channels," *IEEE Trans. Inf. Theory*, vol. 46, no. 7, pp. 2666–2670, Nov. 2000.
- [12] Z. Kukorely and K. Zeger, "The capacity of some hexagonal (d, k) constraints," in *Proc. IEEE Int. Symp. Information Theory*, Washington, DC, Jun. 2001, p. 64.
- [13] —, "Automated theorem proving for hexagonal run length constrained capacity computation," in *Proc. IEEE Int. Symp. Information Theory*, Seattle, WA, Jul. 2006, pp. 1199–1203.
- [14] Z. Nagy and K. Zeger, "Capacity bounds for the hard-triangle modes," in *Proc. IEEE Int. Symp. Information Theory*, Chicago, IL, Jun./Jul. 2004, p. 162.
- [15] —, "Asymptotic capacity of two-dimensional channels with checkerboard constraints," *IEEE Trans. Inf. Theory*, vol. 49, no. 9, pp. 2115–2125, Sep. 2003.
- [16] R. M. Roth, P. H. Siegel, and J. K. Wolf, "Efficient coding schemes for the hard-square model," *IEEE Trans. Inf. Theory*, vol. 47, no. 3, pp. 1166–1176, Mar. 2001.
- [17] M. Schwartz and T. Etzion, "Two-dimensional cluster-correcting codes," *IEEE Trans. Inf. Theory*, vol. 51, no. 6, pp. 2121–2132, Jun. 2005.
- [18] W. Weeks and R. E. Blahut, "The capacity and coding gain of certain checkerboard codes," *IEEE Trans. Inf. Theory*, vol. 44, no. 3, pp. 1193–1203, May 1998.

Secret Key Capacity for Optimally Correlated Sources Under Sampling Attack

Jun Muramatsu, *Member, IEEE*, Kazuyuki Yoshimura, Kenichi Arai, and Peter Davis, *Member, IEEE*

Abstract—The capacity for secret key agreement for permutation-invariant and symmetric sources under a sampling attack is investigated. The supremum of the normalized secret key capacity is introduced, where the supremum is taken over all permutation-invariant sources or all symmetric sources and the normalized secret key capacity is the secret key capacity divided by the description length of the symbol. It is proved that the supremum of the normalized secret key capacity bound under a sampling attack is close to $1/m$ for permutation-invariant sources and $O(1/m)$ for symmetric sources, where m is the number of Eve's sources.

Index Terms—Permutation-invariant source, sampling attack, secret key agreement, secret key capacity, secret key capacity bound, symmetric source.

I. INTRODUCTION

In this correspondence, we consider a situation in which two legitimate parties Alice, Bob, and an eavesdropper Eve have respective correlated sequences which are the outputs of a correlated source. To transmit messages securely, Alice and Bob have to agree on a secret key. Secret key agreement is a procedure for agreeing on a secret key by exchanging messages over a public channel. Maurer [8] defined secret key capacity, which is the least upper bound for the key generation rate of the secret key agreement, and presented an upper and a lower bound for the secret key capacity. Secret key capacity is studied in [1], [3], [9], [13], [4], [5]. It should be noted here that secret key agreement has many variations that have been reported in many papers.

In this correspondence, we consider the situation where a trusted server distributes correlated random sequences to many and unspecified users.

Pairs of users can perform secret key agreement using the random sequences that they obtain from the server. We consider two cases of this situation. In the first case, the server distributes correlated random sequences via secure mutually independent noiseless channels. In the second case, the server broadcasts a random sequence to all users via noisy channels. In this case, the users obtain sequences which have correlations depending on the properties of the noisy channels. This case corresponds to the satellite scenario introduced by Maurer [8]. Formally, this second case is just a special case of the first case.

A critical type of attack in these situations is *sampling attack* whereby Eve obtains more sequences than Alice or Bob to increase her information about the sequences obtained by Alice and Bob. Under sampling attack, the secret key capacity decreases with the number of Eve's samples. In particular, for the source studied in [8], [11], the secret key capacity decreases exponentially as the number of Eve's samples increases. This is obviously a critical shortcoming

Manuscript received December 28, 2005. The material in this correspondence was presented in part at the IEEE International Symposium on Information Theory, Adelaide, Australia, September 2005.

The authors are with the NTT Communication Science Laboratories, NTT Corporation, Kyoto 619-0237 Japan (e-mail: pure@cslab.kecl.ntt.co.jp; kazuyuki@cslab.kecl.ntt.co.jp; ken@cslab.kecl.ntt.co.jp; davis@cslab.kecl.ntt.co.jp).

Communicated by A. Canteaut, Associate Editor for Complexity and Cryptography.

Digital Object Identifier 10.1109/TIT.2006.883552